

## Supporting Information for

### Submillimeter and Lead-free $\text{Cs}_3\text{Sb}_2\text{Br}_9$ Perovskite Nanoflakes: Inverse Temperature Crystallization Growth and Application for Ultrasensitive Photodetectors

Zhi Zheng<sup>1‡</sup>, Qingsong Hu<sup>2‡</sup>, Hongzhi Zhou<sup>3‡</sup>, Peng Luo<sup>1</sup>, Anmin Nie<sup>4</sup>, Haiming Zhu<sup>3</sup>, Lin Gan<sup>1</sup>,  
Fuwei Zhuge<sup>1</sup>, Ying Ma<sup>1</sup>, Haisheng Song<sup>2</sup>, and Tianyou Zhai<sup>1\*</sup>

<sup>1</sup>State Key Laboratory of Material Processing and Die & Mould Technology, School of Materials  
Science and Engineering, Huazhong University of Science and Technology (HUST), Wuhan  
430074, Hubei, P. R. China

<sup>2</sup>Wuhan National Laboratory for Optoelectronics (WNLO) and School of Optical and Electronic  
Information, Huazhong University of Science and Technology (HUST), Wuhan 430074, Hubei, P.  
R. China

<sup>3</sup>Centre for Chemistry of High-Performance and Novel Materials, Department of Chemistry and  
State Key Laboratory of Modern Optical Instrumentation, Zhejiang University, Hangzhou  
310027, Zhejiang, P. R. China

<sup>4</sup>Center for High Pressure Science, State Key Laboratory of Metastable Materials Science and  
Technology, Yanshan University, Qinhuangdao 066004, Hebei, P. R. China

‡ Zhi Zheng, Qingsong Hu and Hongzhi Zhou contributed equally to this work.

Corresponding Authors: \*E-mail: zhaity@hust.edu.cn

## 1. Complementary equations:

1.1 The relation between integral intensity  $I(T)$  and temperature ( $T$ ) is shown as follows:

$$I(T) = \frac{I_0}{1 + A \exp\left(-\frac{E_b}{K_b T}\right)} \quad (1)$$

where  $I_0$  is the integral intensity at 0 K,  $A$  is a parameter of radiative lifetime,  $K_b$  is the Boltzmann constant. For the calculation of  $E_b$ , we plot  $1/I$  as a function of  $1/T$ .

1.2 This temperature dependent FWHM curve could be described by Boson model:

$$\Gamma(T) = \Gamma_0 + \sigma T + \frac{\Gamma_{op}}{\exp\left(\frac{h\omega_{op}}{K_B T}\right) - 1} \quad (2)$$

where  $\Gamma_0$  is the inhomogeneous broadening contribution,  $\sigma$  show the interaction of exciton and acoustic phonon,  $\Gamma_{op}$  describe the exciton and optical phonon interaction,  $h\omega_{op}$  is the optical phonon energy.

1.3 The responsivity of the photodetector is calculated using the following formula:

$$R = \frac{\Delta I}{PS} \quad (3)$$

where  $\Delta I = I_{on} - I_{off}$ ,  $\lambda = 450$  nm,  $P$  is light power, and  $S = 1.0 \times 10^{-6}$  cm $^2$ .

1.4 The detectivity can be described as follows:

$$D^* = \frac{R}{(2qI_{\text{dark}}/S)^{1/2}} \quad (4)$$

where  $q$  is electron charge ( $1.6 \times 10^{-19}$  C),  $I_{\text{dark}}$  is the dark current.

**2. Complementary figures:**

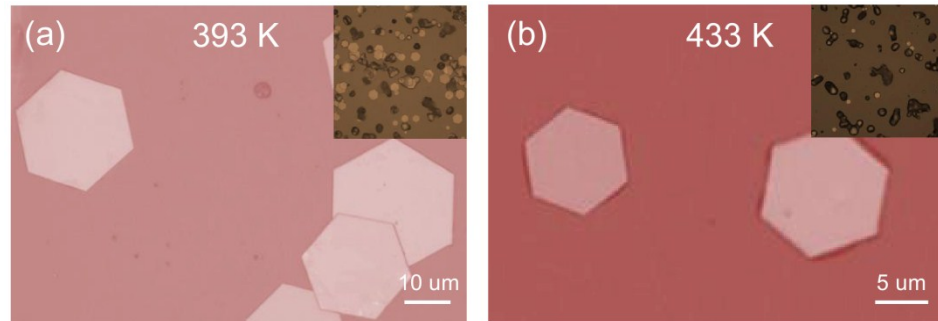


**Fig. S1** (a) Synthesis of CPN at vaporization temperature at 393 K. (b) Synthesis of CPN at vaporization temperature at 433 K.

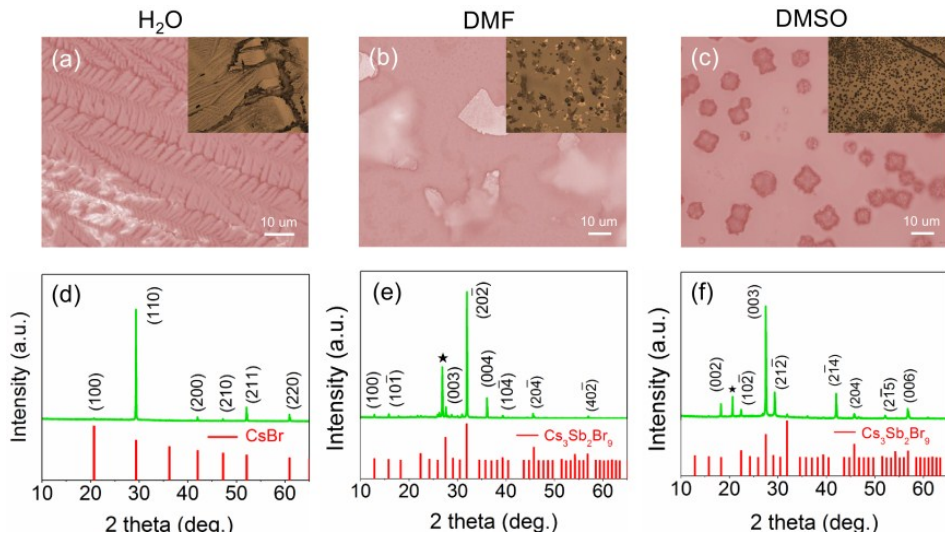


**Fig. S2** (a-c) OM of synthesized CPN using solvent of  $\text{H}_2\text{O}$ , DMF and DMSO, respectively. Inset is the corresponding high magnification OM. (d-f) XRD of synthesized samples using solvent of  $\text{H}_2\text{O}$ , DMF and DMSO, respectively. The peak remarked asterisk is impurity.

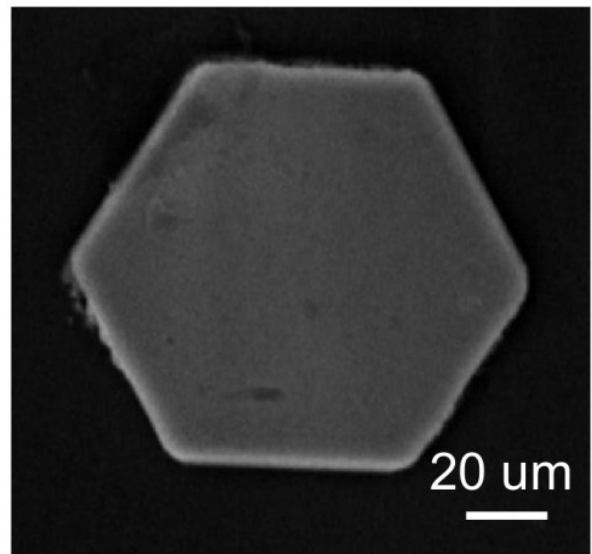


**Fig. S3** SEM image of a typical CPN.

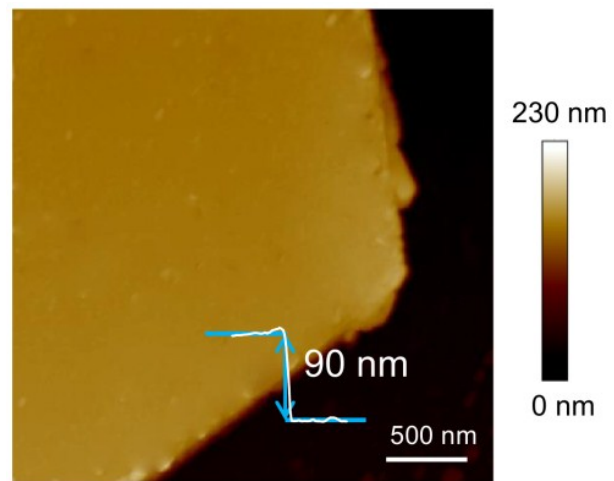


**Fig. S4** AFM image of a typical CPN.

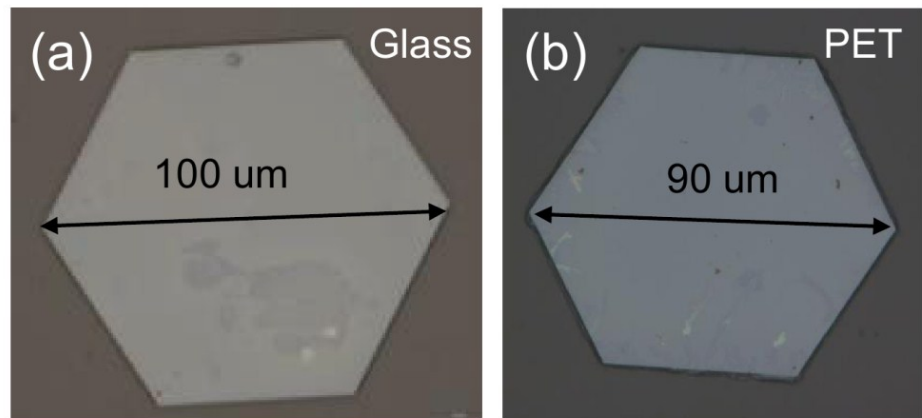


**Fig. S5** (a,b) OM images for CPN growth on substrates of glass, PET.

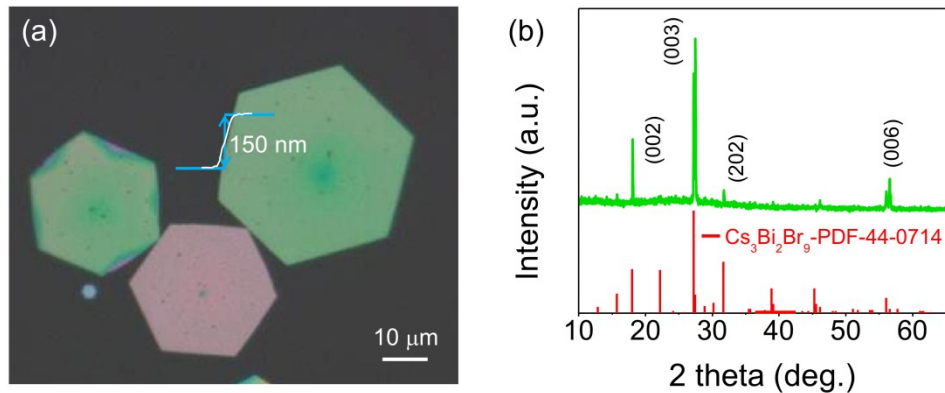


**Fig. S6** (a) OM of  $\text{Cs}_3\text{Bi}_2\text{Br}_9$  nanoflakes, the thickness of a typical nanoflake is 150 nm. (b) XRD patterns for  $\text{Cs}_3\text{Bi}_2\text{Br}_9$  nanoflakes prepared in the HBr/H<sub>2</sub>O hybrid solvent.

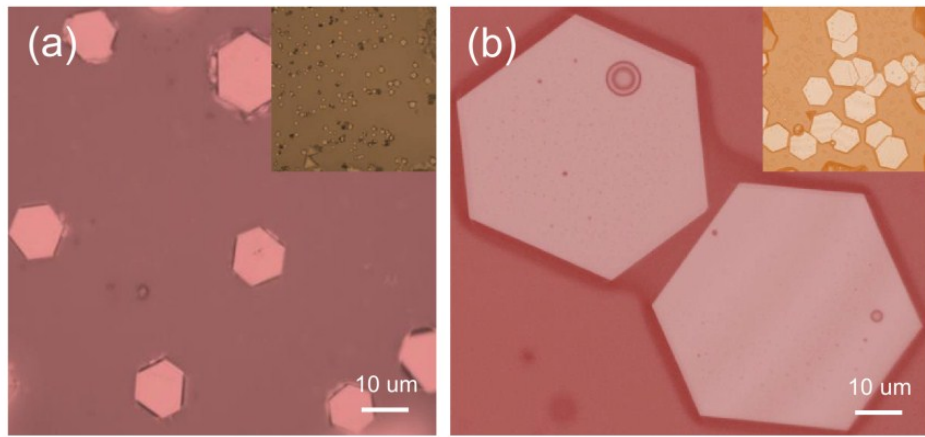


**Fig. S7** Synthesis of CPN at (a) 0.04 mmol/L and (b) 0.12 mmol/L CsBr concentrations, respectively.

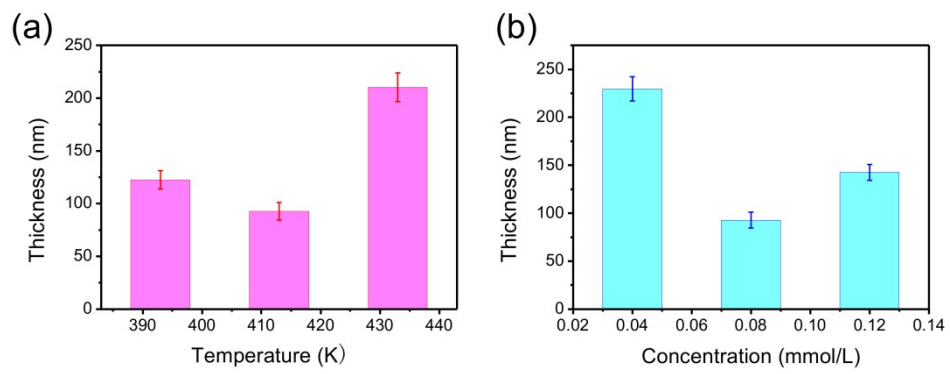


**Fig. S8** Histogram of thickness for CPN synthesized at different temperatures and concentrations.

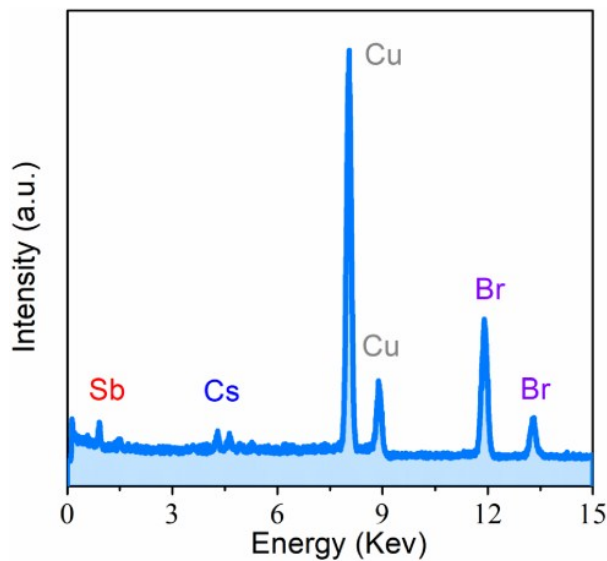


**Fig. S9** EDS curve of CPN.

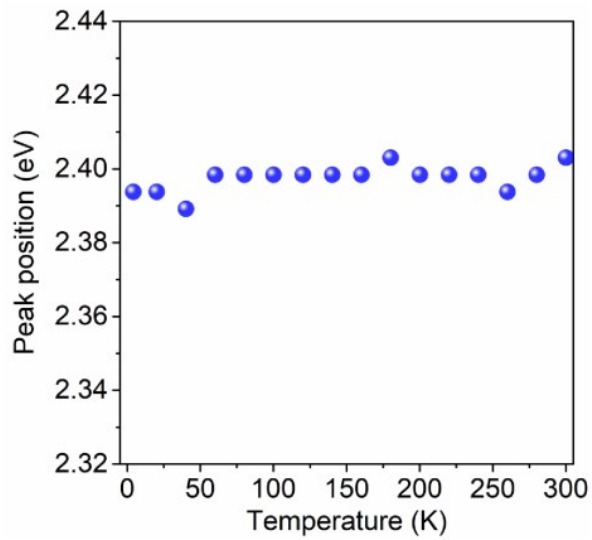


**Fig. S10** Temperature dependence of peak position of PL peaks.

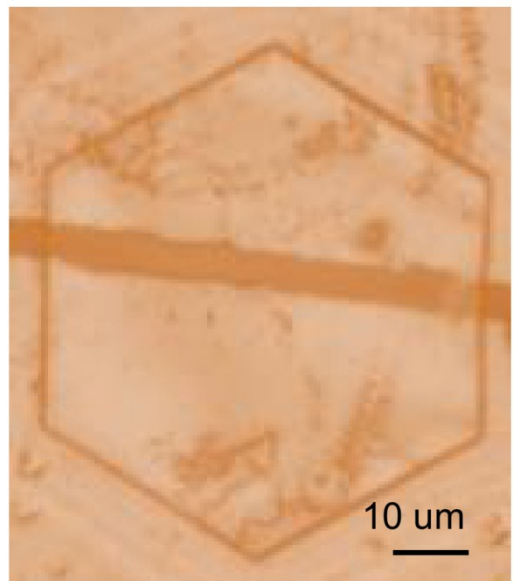


**Fig. S11** OM image of CPN device fabricated via a dry transfer method.

**Table S1.** Comparison of devices based on perovskite nanoplates

Photo detector	On-off ratio	Rise/Decay Time (ms)	Responsivity (A/W)	Detectivity (Jones)	Ref.
Gr/MAPbI <sub>3</sub> /Gr heterostructure	~4	22/37	950	9.6×10 <sup>10</sup>	1
MAPbI <sub>3</sub> monolayer	3000	0.019/0.024	0.64	1.2×10 <sup>12</sup>	2
CsPbBr <sub>3</sub> nanosheets	~100	17.8/29.9	1.9×10 <sup>-4</sup>	2.2×10 <sup>9</sup>	3
CH <sub>3</sub> NH <sub>3</sub> PbI <sub>3</sub> nanoplates	<1	150/150	0.023	1.5×10 <sup>9</sup>	4
CH <sub>3</sub> NH <sub>3</sub> PbI <sub>3</sub> nanosheets	16	20/40	22	1.9×10 <sup>8</sup>	5
CsPbBr <sub>3</sub> monocrystalline film	>1000	0.4/9	2.5	1.1×10 <sup>9</sup>	6
CsPbBr <sub>3</sub> nanosheets	100	0.33/0.42	0.53	7.3×10 <sup>12</sup>	7
Cs <sub>3</sub> Sb <sub>2</sub> Br <sub>9</sub> nanoflakes	450	24/48	3.8	2.6×10 <sup>12</sup>	This work

## References

- 1 H. -C. Cheng, G. M. Wang, D. H. Li, Q. Y. He, A. X. Yin, Y. Liu, H. Wu, M. N. Ding, Y. Huang and X. F. Duan, *Nano Lett.* 2016, **16**, 367.
- 2 J. Z. Song, L. M. Xu, J. H. Li, J. Xue, Y. H. Dong, X. M. Li and H. B. Zeng, *Adv. Mater.* 2016, **28**, 4861.
- 3 L. F. Lv, Y. B. Xu, H. H. Fang, W. J. Luo, F. J. Xu, L. M. Liu, B. W. Wang, X. F. Zhang, D. Yang, W. D. Hu and A. G. Dong, *Nanoscale* 2016, **8**, 13589.
- 4 L. Niu, Q. S. Zeng, J. Shi, C. X. Cong, C. Y. Wu, F. C. Liu, J. D. Zhou, W. Fu, Q. D. Fu, C. H. Jin, T. Yu, X. F. Liu and Z. Liu, *Adv. Funct. Mater.* 2016, **26**, 5263.
- 5 J. Liu, Y. Xue, Z. Wang, Z. Q. Xu, C. Zheng, B. Weber, J. Song, Y. Wang, Y. Lu, Y. Zhang and Q. Bao, *ACS Nano* 2016, **10**, 3536.
- 6 Z. Yang, Q. Xu, X. D. Wang, J. F. Lu, H. Wang, F. T. Li, L. Zhang, G. F. Hu and C. F. Pan, *Adv. Mater.* 2018, **30**, 1802110.
- 7 Z. Yang, M. Q. Wang, H. W. Qiu, X. Yao, X. Z. Lao, S. J. Xu, Z. H. Lin, L. Y. Sun and J. Y. Shao, *Adv. Funct. Mater.* 2018, **28**, 1705908.